Dynamic Optimization of Tendon Tensions in Biomorphically Designed Hands with Rolling Constraints

Marco Gabiccini, Mirko Branchetti, Antonio Bicchi

***Abstract*—Biomorphic structures for robotic manipulation based on tendon-driven mechanisms have been considered in robotic design for several decades, since they provide lightweight end-effectors with high dynamics. Following this trend, many new robot designs have being proposed based on tendon driven systems. Quite noticeably, the most advanced ones include also higher kinematic pairs and unilateral types of constraints.**

In this paper, we present a general framework for modeling the above class of mechanical systems for robotic manipulation. Such systems, including biomorphically designed devices, consist of articulated limbs with redundant tendinous actuation and unilateral rolling constraints. Methods based on convex analysis are applied to attack this broader class of mechanisms, and are shown to provide a basis for the dynamic control of co-contraction and internal forces that guarantee the correct operation of the system, despite limited friction between contacting surfaces or object fragility. An algorithm is described and tested that integrates a computed torque law, and allows to control tendon actuators to "optimally" comply with the prescribed constraints.

I. INTRODUCTION

Human hands are capable of many dextrous grasping and manipulation tasks. Dexterity of movements is achieved in part due to the biomechanics as well as the neuromuscular control [1]. To be able to understand and analyze human level of dexterity, and to achieve it with robotic hands, it is of fundamental importance to correctly model the articular and tendinous structure of the limbs. The extremely low friction in articular joints, due to both the outstanding lubrication properties of synovial fluid and the use of rolling pairs between bone processes, as well as the remotization of actuators made possible by tendon structures, represent the fundamental advantages of biomorphic structures over conventional mechanical designs. Moreover, the redundancy of the tendinous system offers the possibility of *co-contracting* the tendons so as to optimally tune their stiffness, and configure the limbs for different tasks (precision grasp, power grasp, etc.).

Motivated by these advantages, numerous new robot designs are based on tendon driven systems with higher kinematic pairs.

The first one is the Anatomically Correct Testbed (ACT) Hand [2], [3]. Here, the nonlinear interactions between muscles excursions and joint movements are mimicked by human-matching bone shapes, and by the properties of the tendon hood connecting the actuators to the finger bones. A direct muscle position controller and a force-optimized joint controller for joint angle tracking have been implemented for the index finger motion. However, fingertip or contact-point force controller for object interaction is still under investigation.

Another recent design worth of mention is the highly anthropomorphic hand-arm system [4], which is under development at DLR. It consists of a 19−DoF hand and a 7−DoF flexible arm, where fingers are designed as endoskeletons with bionic joints. In particular, the metacarpal joint is designed as a hyperbolically-shaped saddle joint, whereas the interphalangeal finger joints are designed as unilateral hinge joints. In case of overload, the safe dislocation of the *bones* is enabled by the unilateral joints, and is carried by the elasticity of the (tendon) drive train. Intrinsic safety and robustness represent other advantages of this biomorphically inspired design [5], [6].

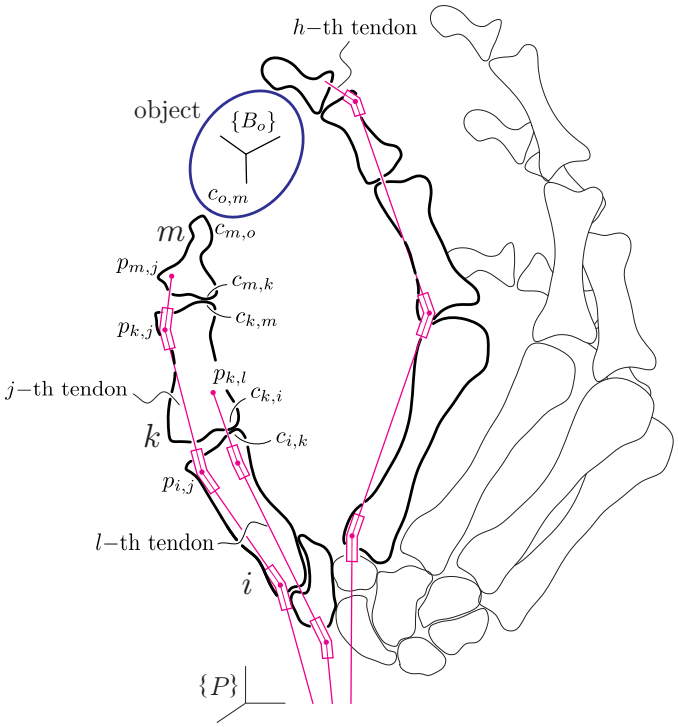

Fig. 1: Biomorphically designed tendinous system.

General analyses of tendon driven mechanisms have been attempted in most cases for systems where tendons are routed through joints by means of pulleys, see e.g. [7]. More general configurations composed by nets of tendons and actuators were presented in [8], while dexterity measures under unilateral constraint imposed by tendons were investigated in [9].

In another context, the motion control of a multi-DoF tendon-driven manipulator by optimizing the tension distribution was investigated in [10]. The algorithm here proposed allowed for a reduction of energy consumption by the actuators while not hindering the tracking capability.

More complex tendon-actuated structures have been considered mainly in the biomechanical literature, see e.g. [11] and [12], to mention only a few.

In this paper, we propose a unified approach to model and control a wide variety of configurations that can be

This work is supported by the European Commission under CP grant no. 248587, "THE Hand Embodied", within the FP7-ICT-2009-4-2-1 program "Cognitive Systems and Robotics".

M. Gabiccini is with the Department of Mechanical, Nuclear and Production Engineering, University of Pisa, 56122 Pisa, Italy m.gabiccini@ing.unipi.it

M. Branchetti and A. Bicchi are with the Interdepartmental Research Center "E. Piaggio", University of Pisa, 56122 Pisa, Italy {m.branchetti, bicchi}@centropiaggio.unipi.it

encountered in biological systems or conceived for artificial devices. For the widest generality, we model articulated limbs with tendinous actuation and manipulated object/objects as a collection of rigid bodies, interacting through generalized virtual springs. The end points of the springs are allowed to move over the object boundaries, thus simulating rolling motions. Distinction between manipulator *links* and *objects* to be manipulated is not intrinsic to the model, and can be recovered in the final stage of the analysis. Since contacts between any of the bodies with any of the others are allowed, whole-limb manipulation is naturally investigated within this framework.

A dynamic force distribution analysis in contacts and tendons is proposed, with generalizes the approach presented in [13]. As a result, we propose a control law that allows the manipulated object to track a specified motion while ensuring the integrity of the system by application of proper tendon tensions. The actual choice of the tendon actions on the system is eventually made on the basis of an optimality criterion that embodies the fulfilment of physical constraints (fragility of the object, friction limits in the contact interfaces, allowable tendon tension ranges, etc.). A numerical implementation of the overall methodology is presented for a three-fingered tendon-driven hand, with unilateral rolling constraints among the limbs, manipulating an object. Each finger has one 2-DoF saddle joint and two 1-DoF unilateral hinge joints, and was inspired by the design of the new DLR hand-arm system. Many issue related to real-world implementation of the above strategies, like robustness to modeling errors and stochasticity, need still to be investigated and suggest future research directions. However, promising simulation results show that the proposed methodology could help in implementing more easily biological strategies for the unified position and force control of complex biomorphic structures.

II. SYSTEM DESCRIPTION

A. Preliminaries

For the widest generality, we model tendon-actuated robotic structures as a collection of an arbitrary number n of rigid bodies that may be connected one with any of the others, or with the environment, through revolute or prismatic joints, and unilateral rolling contacts. Bodies are numbered from 1 to n, while the environment is assigned the index 0. A schematic of such a structure is depicted in Fig. 1.

According to the usual practice, we consider a fixed (palm) frame $\{\mathsf{P}\}$, and we attach a barycentric frame $\{\mathsf{B}_i\}$ to the $i-$th object in the system, $(i = 1, \dots, n)$. We denote with $g_{PB_i} \in \mathrm{SE}(3)$ the posture of $\{\mathsf{B}_i\}$ with respect to $\{P\}$, and we employ the Product of Exponentials (PoE) formula [14] for its parametrization, i.e.

$$g_{PB_i}(\theta_i) = \left(\prod_{j=1}^{6} e^{\widehat{\xi}_{ij}\theta_{ij}} \right) g_{PB_i}(0). \tag{1}$$

This choice is motivated by the recognized superiority of this approach over conventional Denavit-Hartenberg parametrizations [15]. Here, the $\widehat{\xi}_{ij}$'s form a basis for $\mathfrak{se}(3)$, the Lie algebra of rigid body motions, $\theta_i = [\theta_{i1} \cdots \theta_{i6}]^T$ are the exponential coordinates of the 2nd kind [16] for a local representation of $\mathrm{SE}(3)$ for the $i-$th body, and $g_{PB_i}(0)$ is its initial configuration. We cast the set of local parametrizations for all the objects in the vector $\theta = [\theta_1^T \cdots \theta_n^T]^T$.

For each pair (i, k) of connected bodies we define $\{\mathsf{C}_{i,k}\}$ and $\{\mathsf{C}_{k,i}\}$ as the *normalized Gauss frames* with origin in the common contact point, fixed to the $i-$th and $k-$th body, respectively. The local frames are chosen so that the $x-$ and $y-$axes span the local tangent plane to the body surface, and the $z-$axis is aligned with the outward normal. The components of the common origin of frames $\{\mathsf{C}_{i,k}\}$ and $\{\mathsf{C}_{k,i}\}$ are denoted as $c_{i,k}$ and $c_{k,i}$, depending on whether they expressed in $\{\mathsf{B}_i\}$ or $\{\mathsf{B}_k\}$, respectively.

B. Actuation system

The actuation system modelled consists of q motors and r tendons. Tendons have always one end fixed to one object, while the other end may be connected to a motor or to another object, therefore $r \geq q$. Tendons may be routed through idle pulleys or sheaths. With reference to Fig. 1, we denote with $p_{i,j}$ the point on the $i-$th body where the $j-$th tendon is fixed or is passed through. Actuators are placed remotely on the environment, therefore the position of the $j-$th tendon actuator is denoted by $p_{0,j}$. Under the assumption of a frictionless transmission system, the tendons can be considered uniformly stressed, and the tensions can be collected in a vector $t = [t_1 \cdots t_r]^T \in \mathbb{R}^r$. Denoting with ${}^tF_{ij}^{B_i} \in \mathbb{R}^6$ the components in $\{B_i\}$ of the wrench exerted on the $i-$th object by the $j-$th tendon, it is possible to write

$${}^tF_{ij}^{B_i} = T_{ij}^{B_i} t_j, \quad T_{ij}^{B_i} = \mathrm{Ad}_{g_{B_iP}}^{-T} T_{ij}^{P}, \tag{2}$$

where Ad_g is the adjoint operator of the element g, and the explicit expressions of T_{ij}^P (given in the appendix) depend on the tendon net topology. The effect on the $i-$th object of the whole tendon net can be written in matrix form as follows

$${}^tF_i^{B_i} = T_i^{B_i} t, \quad T_i^{B_i} = [T_{i1}^{B_i} \cdots T_{ir}^{B_i}] \in \mathbb{R}^{6\times r}. \tag{3}$$

Then, by stacking eq. (3) for all the objects, the overall effect of the tendons on the articulated structure can be cast as

$${}^tF^B = Tt, \quad T = [{T_1^{B_1}}^T \cdots {T_n^{B_n}}^T]^T, \tag{4}$$

where ${}^tF^B \in \mathbb{R}^{6n}$, and $T \in \mathbb{R}^{6n\times r}$.

To consider that not all the tendons are directly actuated, a suitable selection matrix $\Gamma \in \mathbb{R}^{q\times r}$ is introduced. This maps tendon tensions $t \in \mathbb{R}^r$ to active forces $\tau \in \mathbb{R}^q$ applied on tendons by the q motors as follows

$$\tau = \Gamma t, \tag{5}$$

where $\Gamma_{ij} = 1$ if the $j-$th tendon is directly connected to the $i-$th motor, and $\Gamma_{ij} = 0$ otherwise.

The model of tendon elasticity can be obtained by introducing the relative displacement δx_t between the tendon ends. This is due to both a change in the configuration of the bodies and a displacement δq of the tendon ends imposed by the motors. By duality arguments, it is easy to show that δx_t has the following form

$$\delta x_t = T^T J^B \delta\theta - \Gamma^T \delta q, \tag{6}$$

where J^B is a matrix obtained by properly combining the distal Jacobians of all the bodies, i.e. $J^B = \mathrm{blkdiag}(J_{PB_1}^{B_1}, \dots, J_{PB_n}^{B_n})$. Accordingly, and assuming a linear elasticity model for each tendon, the vector of tensions can be recovered as

$$t = K_t\, \delta x_t + \hat{t}, \tag{7}$$

where $\hat{t}$ accounts for preload tensions in the reference configuration, and $K_t = \mathrm{diag}(k_1, \dots, k_r) \in \mathbb{R}^{r\times r}$ is the stiffness matrix whose entries k_t depend on the elastic characteristics of the tendons.

C. Contact force model

To model the constraint reactions due to joints and/or unilateral rolling contacts between connected bodies, a *penalty formulation* is adopted. In this framework, elastic reaction forces are generated in the directions not allowed by the type of connection. Considering contact between the $i-$th and $k-$th body, the components (in $\{\mathsf{C}_{k,i}\}$) of the constrained relative displacement of k with respect to i, i.e. $\delta C_{ik}^{C_{k,i}} = B_{i,k}^T(\delta C_k^{C_{k,i}} - \delta C_i^{C_{k,i}})$ can be expressed as

$$\delta C_{ik}^{C_{k,i}} = B_{i,k}^T(J_{PB_k}^{C_{k,i}}\delta\theta_k - J_{PB_i}^{C_{k,i}}\delta\theta_i), \tag{8}$$

where $B_{i,k} \in \mathbb{R}^{6\times c}$ is a basis for the contact wrench, or, equivalently, $B_{i,k}^T$ selects the relative displacement constrained by the connection. As an example, $c = 4$ for a soft-finger (SF) contact. Under the assumptions of a linear elastic characteristic, the contact force exerted by the $k-$th on the $i-$th body can be expressed as follows

$$f_{ki}^{C_{k,i}} = K_{i,k}\,\delta C_{ik}^{C_{k,i}} + \hat{f}_{ki}^{C_{k,i}}, \quad f_{ki}^{C_{k,i}} \in \mathbb{R}^c, \tag{9}$$

where $K_{i,k} \in \mathbb{R}^{c\times c}$ encodes the characteristics of the contact interface (virtual springs), and $\hat{f}_{ki}^{C_{k,i}}$ models the preload contact force which can be present in the reference configuration. Then, the components in the barycentric frame $\{\mathsf{B}_i\}$ of the full wrench exerted by k on i, are easily obtained as

$${}^cF_{ki}^{B_i} = G_{ki}\,f_{ki}^{C_{k,i}}, \quad G_{ki} = \mathrm{Ad}_{g_{B_iC_{k,i}}}^{-T} B_{i,k}. \tag{10}$$

The resultant wrench on the $i-$th body due to contacts depends on its connectivity with the other objects. By introducing the list $\nu(i)$ as a mean to encode the connectivity of the $i-$th body with all the others, and the shorthand notation $G_i = [G_{ki}]_{k\in\nu(i)}$ to represent proper juxtaposition in columns/rows of matrices or vectors, we can write

$${}^cF_i^{B_i} = G_i\,f_i^{C_{\#,i}}, \tag{11}$$

where, $f_i^{C_{\#,i}} = [f_{ki}^{C_{k,i}}]_{k\in\nu(i)}$, is comprised of all the contact force components (each one in its contact frame) exerted on body i by its connected neighbours.

Then, in order to avoid redundancy and reduce the dimensionality of the system, we count the contact force components only once by introducing the global contact force vector $f \in \mathbb{R}^s$ as follows

$$f = \bigcup_{i=1}^{n} f_i^{C_{\#,i}}. \tag{12}$$

According to the above definition, the overall contact wrench contribution ${}^cF^B$ can be written as

$${}^cF^B = G\,f, \tag{13}$$

where matrix $G \in \mathbb{R}^{6n\times s}$ can be extracted by inspection or by automatic search procedures from the set (obtained for $i = 1, ..., n$) of eq. (11) and making use of eqs. (12) and (13).

D. Dynamic evolution of the contact points

We assume that the contact points between connected bodies move over their respective surfaces in response to a relative twist, according to pure rolling (only $\omega_x \neq 0$ and $\omega_y \neq 0$) between rigid surfaces. The update law for the local coordinates of the surfaces are based on Montana's equations [17], which are here specialized for the case of contact between bodies i and k:

$$\begin{bmatrix}\dot{\alpha}_{k,i}\\ \dot{\alpha}_{i,k}\end{bmatrix} = \begin{bmatrix} M_{k,i}^{-1}(K_{k,i} + \tilde{K}_{i,k})P \\ M_{i,k}^{-1}R_\psi(K_{k,i} + \tilde{K}_{i,k})P\end{bmatrix}\begin{bmatrix}\omega_{x_{i,k}}\\ \omega_{y_{i,k}}\end{bmatrix},$$
$$\dot{\psi}_{i,k} = [T_{k,i}M_{k,i} \quad T_{i,k}M_{i,k}]\begin{bmatrix}\dot{\alpha}_{k,i}\\ \dot{\alpha}_{i,k}\end{bmatrix} \tag{14}$$

It is worth recalling that $\alpha_{k,i}$ and $\alpha_{i,k}$ are the Gaussian coordinates of the contact point for the surfaces k and i, respectively, while $\psi_{i,k}$ is the angle that aligns $x_{i,k}$ onto $x_{k,i}$ with a CCW rotation about the $z_{k,i}-$axis. The main assumption here is that we neglect the variation of the surface *metric, curvature and torsion forms*, M, K and T due to contact deformation, and we assume a rigid model for the mating surfaces.

It can be useful to show that the components of the relative rolling velocity can be easily computed as

$$\begin{bmatrix}\omega_{x_{i,k}}\\ \omega_{y_{i,k}}\end{bmatrix} = {B_{i,k}^{(a)}}^T\big(J_{PB_k}^{C_{k,i}}\dot{\theta}_k - J_{PB_i}^{C_{i,k}}\dot{\theta}_i\big), \tag{15}$$

where $B_{i,k}^{(a)}$ is a basis for $\mathcal{N}(B_{i,k}^T)$, or, equivalently, ${B_{i,k}^{(a)}}^T$ selects the components of the relative twist $V_{B_iB_k}^{C_{k,i}}$ that are not constrained by the type of contact.

E. Overall system model

According to the definitions and notations introduced above, the model of the system can be summarized by the following set of matrix equations:

$$F^B = [G \quad T]\begin{bmatrix}f\\ t\end{bmatrix} =: \bar{G}\bar{f}, \tag{16}$$

$$F^B = M(\theta)\ddot{\theta} + C(\theta,\dot{\theta})\dot{\theta} + N(\theta) \tag{17}$$

$$\tau = \Gamma\,t, \tag{18}$$

$$\bar{f} = \bar{K}\begin{bmatrix}\bar{G}^T J^B & -\bar{\Gamma}^T\end{bmatrix}\begin{bmatrix}\delta\theta\\ \delta q\end{bmatrix} + \hat{\bar{f}} =: M\begin{bmatrix}\delta\theta\\ \delta q\end{bmatrix} + \hat{\bar{f}}, \tag{19}$$

beside eqs. (14) and (15) for each pair (i, k) of connected bodies. Eq. (16) is the set of wrenches on the system objects, eq. (17) describes the overall system dynamics, eq. (18) relates the tendon tensions with the actuator forces, and eq. (19) encodes the constitutive models for contact forces and tendon tensions. In eq. (19), matrix $\bar{G} \in \mathbb{R}^{6n\times(s+r)}$ is defined as in (16), and $\bar{\Gamma} = [0 \quad \Gamma] \in \mathbb{R}^{q\times(s+r)}$. The overall stiffness matrix $\bar{K} \in \mathbb{R}^{(s+r)\times(s+r)}$ is defined as $\bar{K} = \mathrm{blkdiag}(K_c, K_t)$, where K_c can be elicited from (9) and K_t was defined in (7). It is worth pointing out that matrices M, C and N are formed by appropriately stacking the quantities obtained for the individual objects

$$M = \mathrm{blkdiag}(M_1, \ldots, M_n), \quad C = \mathrm{blkdiag}(C_1, \ldots, C_n),$$
$$N = [N_1^T \cdots N_n^T]^T \tag{20}$$

III. FORCE DISTRIBUTION

The force distribution problem consists in describing the general solution of eq. (16), given the (to be applied) global wrench F^B. Under the technical condition (usually ensured by a proper design) that $\mathcal{R}(\bar{G}) = \mathbb{R}^{6n}$, the actuator actions can exert any prescribed wrench. In this case, the general solution of eq. (16) can be written as the sum of (i) a particular solution, and (ii) a homogeneous one.

A. Particular solution

By following arguments similar to those presented in [13], given an equilibrium configuration $\hat{\theta}$ under a set of external loads $\hat{F}^B$, with contact and tendon forces $\hat{\bar{f}}$, the additional forces $\delta\bar{f}_p$ to be applied if an additional load δF^B is prescribed (with $\delta q = 0$) are

$$\delta\bar{f}_p = \bar{G}^R_{\bar{K}}\delta F^B, \quad \bar{G}^R_{\bar{K}} = \bar{K}\bar{G}^T(\bar{G}\bar{K}\bar{G}^T)^{-1} \tag{21}$$

It is worth noting that, among the infinitely many right inverses of $\bar{G}$, only the $\bar{K}-$weighted right inverse $\bar{G}^R_{\bar{K}}$ is physically motivated, since it returns the contact force distribution associated to the minimum elastic energy stored in the system [18]. Therefore, the particular solution has the general structure $\bar{f} = \hat{\bar{f}} + \delta\bar{f}_p$, with $\delta\bar{f}_p$ obtained in (21).

B. Homogeneous solution

The homogeneous solution of (16) represents connection forces and tendon tensions that do not produce a net wrench on the system. These forces and tensions are referred to as *internal*, and their management is of fundamental importance in grasp planning to avoid separation or slippage in unilateral and rolling pairs. According to eq. (16), it is easy to show that internal forces $\delta\bar{f}_h$[1] must belong to $\mathcal{N}(\bar{G})$. However, since contact forces and tendon tensions are related to the system configuration $\delta\theta$ and the commanded (motor) inputs δq through eq. (19), only those in $\mathcal{R}(M)$ can be obtained. This implies that the system configuration and the motor positions must fulfil the following condition

$$\bar{G}M\begin{bmatrix}\delta\theta\\ \delta q\end{bmatrix} = 0. \tag{22}$$

Let $B \in \mathbb{R}^{(6n+q)\times b}$ be a matrix whose columns span $\mathcal{N}(\bar{G}M)$, whose dimension is b. Then, the subspace of active internal forces $\mathcal{F}_{ha}$ is given by $\mathcal{R}(MB)$. If we introduce the basis matrix $E \in \mathbb{R}^{(s+r)\times e}$, obtained by using only the independent columns of MB, i.e. $E = \text{colbasis}(MB)$, it is possible to give the following definition

$$\mathcal{F}_{ha} = \{\delta\bar{f}_{ha} : \delta\bar{f}_{ha} = Ey, y \in \mathbb{R}^e\}, \tag{23}$$

where y is a free parameter. Note that, among active internal forces and tensions, it is also possible to further distinguish the set of *co-contraction* tensions, as a subspace of $\mathcal{F}_{ha}$ that do not change the contact forces between links and the manipulated object.

Moreover, is it possible to identify passive (preload) internal forces as those that cannot be actively controlled by means of motor displacements. In systems with tendinous structure and rolling pairs, these can be used to model the effects of articular ligaments.

For brevity, in the subsequent application of the methodology, both co-contraction tensions and passive internal forces will not be characterized further, since we will assume that: (i) no pre-loading is present in the system, and (ii) there is no interest in distinguishing between link-to-link and link-to-object forces, but only to ensure the global integrity of the structure in tracking a specified motion.

[1]The subscript h refers to the homogeneous nature of the solution.

IV. OPTIMIZATION OF TENDON TENSIONS

Assuming that the system is not preloaded, the results presented in sec. III allow us to write the general solution of (16) as follows

$$\bar{f} = \bar{G}^R_{\bar{K}}F^B + E\,y \tag{24}$$

where the free vector y parameterizes the active internal forces and tensions, and plays a key role in fulfilling the system constraints.

Following the approach of [19], the limit values of contact constraints for the $(i,j)-$th connection can be profitably written in the generalized form

$$\sigma_{i,j,k} = \alpha_{i,j,k}\|f_{i,j}\| + \beta_{i,j,k}\|m_{i,j}\| + \gamma_{i,j,k}f_{z_{i,j}} + \delta_{i,j,k} \le 0, \tag{25}$$

where the numerical values for various constraint types $(k = 1,2,3)$ are reported in Table I, and where $\alpha_{i,j,3} = (1+\mu_{i,j}^2)^{-1/2}$ and $\beta_{i,j,3} = 1/\mu_{i,j}$. A similar, but simpler, form can be conceived also to describe the bound constraints on the $h-$th tendon tension

$$\nu_{h,l} = \rho_{h,l}\,t_h + \eta_{h,l} \le 0, \tag{26}$$

where the numerical values for the two bounds $(l = 1,2)$ are reported in Table II.

Let ${}^c\Omega_{i,j,k}$ and ${}^t\Omega_{h,l}$ represent the sets of the free parameter y that, for a given global wrench F^B, satisfies the constraints (25) and (26), respectively, with a small positive margin κ. More precisely, let us define ${}^c\Omega_{i,j,k} := \{y : \sigma_{i,j,k} < -\kappa\}$ and ${}^t\Omega_{h,l} := \{y : \nu_{h,l} < -\kappa\}$. The region where all the constraints are satisfied is given by ${}^c\Omega \cap {}^t\Omega$, with

$${}^c\Omega = \bigcap_{i,j,k} {}^c\Omega_{i,j,k}, \quad {}^t\Omega = \bigcap_{h,l} {}^t\Omega_{h,l}. \tag{27}$$

In eq. (27), $i = 1,...,n$, $j \in \nu(i)$, $k = 1,...,3$, $h = 1,...,r$, and $l = 1,2$. For the $(i,j)-$th connection ($k-$th constraint) consider the cost function

$${}^cV_{i,j,k}(y,F^B) = \begin{cases}(2\sigma_{i,j,k})^{-1} & : \quad y \in {}^c\Omega_{i,j,k}\\ a\sigma_{i,j,k}^2 + b\sigma_{i,j,k} + c & : \quad y \notin {}^c\Omega_{i,j,k}\end{cases} \tag{28}$$

and for the $h-$th tendon ($l-$th constraint) consider the cost function

$${}^tV_{i,j,k}(y,F^B) = \begin{cases}(2\nu_{h,l})^{-1} & : \quad y \in {}^t\Omega_{h,l}\\ a\nu_{h,l}^2 + b\nu_{h,l} + c & : \quad y \notin {}^t\Omega_{h,l}\end{cases} \tag{29}$$

Then we form the overall cost function as

$$V(y,F^B) = \sum_{i,j,k} {}^cw_{i,j,k}\,{}^cV_{i,j,k} + \sum_{h,l} {}^tw_{h,l}\,{}^tV_{h,l}, \tag{30}$$

where ${}^cw_{i,j,k}$ and ${}^tw_{h,l}$ are positive weights. By arguments similar to those used in [19], here omitted for brevity, it can be shown that for $\kappa > 0$, and with the choice $a = 3/(2\kappa^4)$,

Constraint type	$\alpha_{i,j,k}$	$\beta_{i,j,k}$	$\gamma_{i,j,k}$	$\delta_{i,j,k}$
Max. force module $(k=1)$	1	0	0	$-f_{i,j}^{\max}$
Min. normal force $(k=2)$	0	0	-1	$f_{z_{i,j}}^{\min}$
Friction cone $(k=3)$	$\alpha_{i,j,3}$	$\beta_{i,j,3}$	-1	0

TABLE I: Force constraint coefficients.

Constraint type	$\rho_{h,l}$	$\eta_{h,l}$
Max. tension ($l=1$)	1	$-t_h^{\max}$
Min. tension ($l=2$)	-1	$t_h^{\min}$

TABLE II: Tension constraint coefficients.

$b = 4/\kappa^3$, and $c = 3/\kappa^2$, the overall cost function $V(y, F^B)$ is twice continuously differentiable and globally strictly convex with respect to $y \in \mathbb{R}^e$. Therefore, standard techniques can be employed to search the unique minimizer $y^\star$, where

$$y^\star = \operatorname{argmin} V(y, F^B). \tag{31}$$

For instance, also the basic Newton-Raphson update law

$$\dot{y}(t) = -\zeta \, (\partial_y^2 V)^{-1} \partial_y V \tag{32}$$

with $\zeta > 0$, provides a globally asymptotically convergent algorithm. More advanced techniques, either based on line search or trust-region strategies, can be devised which provide better convergence performances, see, e.g. [20], for more details. From the numerical optimization perspective, the proposed procedure is to be annoverated among the weighted barrier algorithms [21], which have been proved to be more efficient than standard SDP algorithms [22].

V. CONTROL

In this section, we consider the problem of controlling the position and orientation of an object in $\mathbb{E}^3$ grasped by a biomorphically inspired hand through the appropriate application of tendon tensions. The following considerations are in order: (i) *tracking* – we would like the object to follow a specified trajectory in $SE(3)$ asymptotically, and (ii) *mantaining integrity of the system* – over the entire trajectory we need to produce contact forces and tendon tensions which comply with the constraint limits in the form (25) and (26). It is worth observing that the analysis is here limited to the determination of set-point values for the tendon tensions. Potential hurdles with real-world implementation, like time constants associated to the activation and coordination of the tendons, are not considered here.

A. Overall reference trajectory

Since distinction between hand limbs and object to be manipulated is not intrinsic to our model, we can recover it in this final stage of the analysis when the object task has to be specified. Let $\theta_o^r(t) \in \mathbb{R}^6$ be the object reference trajectory to be tracked. For a manipulating hand properly design to accomplish the task, it is always possible to find the overall system trajectory $\theta^r(t) \in \mathbb{R}^{6n}$ by integrating the differential inverse kinematics

$$\dot{\theta}^r(t) = B(t)\dot{\theta}_o^r(t), \quad B(t) \in \mathbb{R}^{6n \times 6}, \tag{33}$$

where $B(t)$ is reminiscent of the notation employed in the *embedding technique* for multibody dynamic simulations [23].

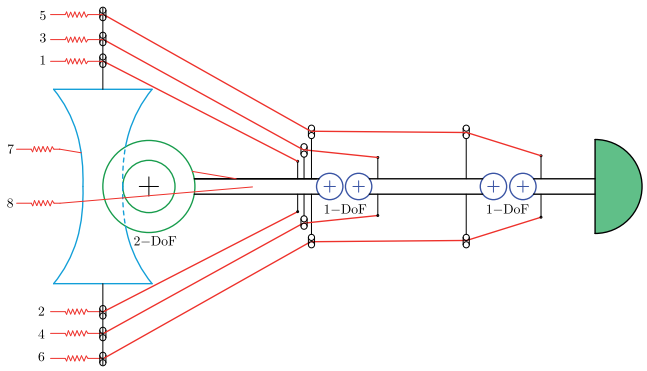

Fig. 2: Schematic of the three-phalanx/eight-tendon finger with one $2-$DoF hyperboloidic (saddle) joint and two $1-$DoF cylindrical rolling joints.

B. Proposed control law

In order to track the desired object trajectory a computed torque control law is proposed for the global wrench:

$$F^B = M(\theta)(\ddot{\theta}^r - K_v\dot{e} - K_p e) + C(\theta, \dot{\theta})\dot{\theta} + N(q). \tag{34}$$

Then, at a generic instant $\check{t}$, when $F^B = \check{F}^B$, contact forces and tendon tensions satisfying the constraints are found (if the problem is feasible) as

$$\check{\tilde{f}} = \begin{bmatrix} \check{f} \\ \check{t} \end{bmatrix} = \bar{G}_K^R \check{F}^B + E\, y^\star, \tag{35}$$

where $y^\star$ is found by integrating the differential law (32). Hence, the necessary actuator forces are recovered as

$$\check{\tau} = \Gamma \check{t}. \tag{36}$$

It is worth noting that the discrete time analog of eq. (32) is straightforward to derive. The only warning to give, however, is that global asymptotic convergence of the algorithm can be proven only for ζ smaller that a limiting value, that allows the convergence only to a finite neighborhood of the optimal grasp.

VI. TEST CASE

A. Hand layout

A hand with three $4-$DoF fingers manipulating a spherical object is considered. Kinematically, each finger consists of three limbs in rolling contact. In particular, the first one is in contact with the environment (metacarpal bones, in the human hand) through one $2-$DoF hyperboloidic (saddle) joint, while the first and the second one, as well as the second and the third one, are in contact through two $1-$DoF cylindrical rolling joints, as shown in Fig. 2. It is worth observing that the mating hyperboloids in the first joint are in point contact, while the cylindrical surfaces of the rolling joints are in line contact: however, both constraints are of unilateral nature and require suitable tendon tensions in order to avoid dislocation or slippage. Contact with the manipulandum happens through a spherical fingerpad that is attached at the end of each finger. Analytically, the contact is modeled as a soft-finger.

The actuation system of each finger is comprised of eight tendons with numbering and routing depicted in Fig. 2. Tendons 1, 3 and 5, and 2, 4 and 6, control the movements of flexion and extensions, respectively. Tendons 7 and 8 account for adduction/abduction movements of the entire structure.

B. Simulation

In order to track a prescribed trajectory (33), and to ensure the integrity of the structure (expressed in the form of inequalities (25) and (26)), the to be applied tendon tensions are computed as in (35). The proposed control law, as well as a simulator of the whole system, has been implemented in MATLAB/Simulink, and has been used to produces *movies* of the dynamic simulations for several reference trajectories.

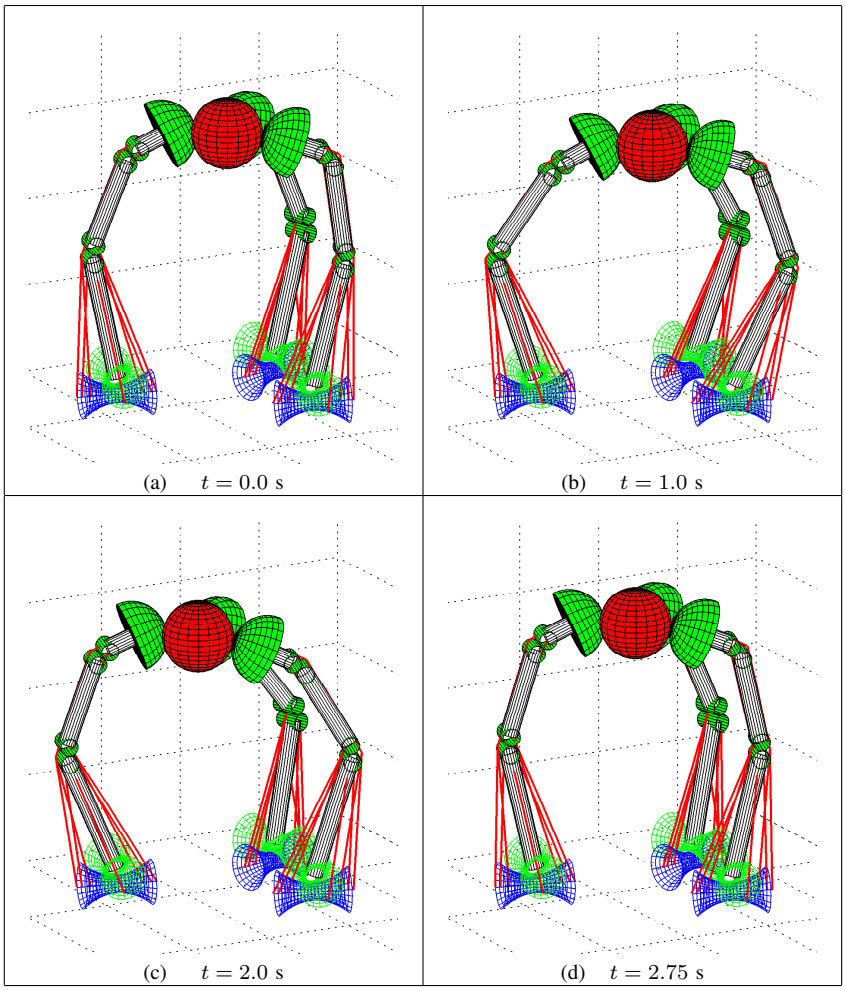

Fig. 3: Four frames from a movie showing the 3-D manipulation of a spherical object by three fingers with spherical fingerpads; overall simulation time $t = 3$ s.

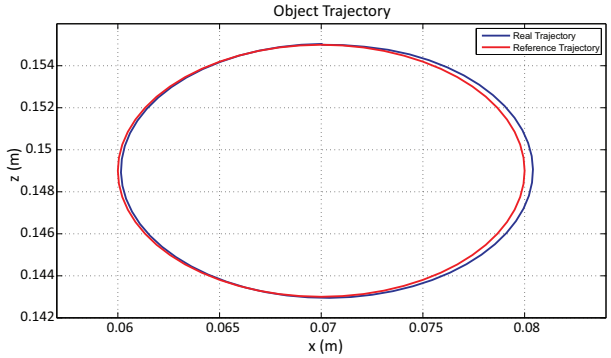

Fig. 4: Reference (blue, dashed) and actual trajectory (red, continuous) of the object barycenter.

Some frames from a simulation movie are reported in Fig. 3. Here, the desired trajectory of the object barycenter is an ellipse in the vertical plane, with constant roll-pitch-yaw angles. Fig. 4 shows the tracking performances for an overall simulation time of 3 s.

For brevity, only the tension for the third finger are presented. In Fig. 5 the control tensions for tendons 1 and 3 are depicted, while in Fig. 6 the values for tendons 2 and 4 to 8 are illustrated.

It is worth observing that the tensions in tendons 1 and 3 (flexion) are one order of magnitude higher than in the corresponding antagonistic tendons 2 and 4 to 8 (extension and adduction/abduction).

As clear from Fig. 5 and 6, all values comply with the constraint $t > t^{\min} = 0.1N$. Even if not explicitly presented for conciseness, all values of the contact forces, both in the unilateral joints and in the fingerpads/object contacts, fulfil the constraints indicated in Table I.

VII. CONCLUSION AND FUTURE WORK

We presented a method for the dynamic analysis and optimal control of the forces needed to balance a mechanical structure, composed by an arbitrary combination of tendons and rigid bodies in contact. The method is very general and allows practically to model a broad variety of configurations, as those encountered in biological systems.

A numerical example has been presented to show the performances of the proposed algorithm in controlling the tendon tensions of a robotic hand with biomorphic fingers during the dynamic manipulation of an object.

Although we only considered tendons and contacts with *linear* stiffness, the method could be modified to cope with

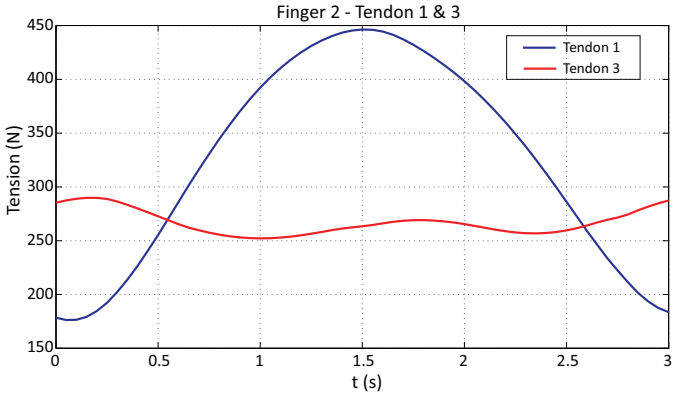

Fig. 5: Tendon tensions for the third finger: tendon 1 and 3; units [N].

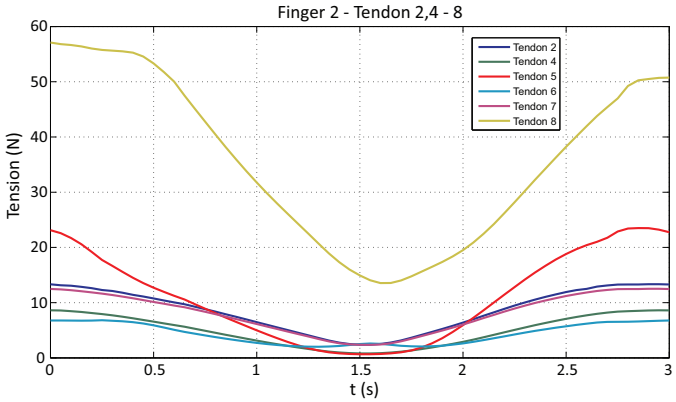

Fig. 6: Tendon tensions for the third finger: tendon 2, 4 – 8; units [N].

variable stiffness characteristics of system components. These would allow the simultaneous control of the trajectory and the workspace stiffness of the manipulated object, while ensuring the observance of the necessary constraints.

VIII. ACKNOWLEDGEMENTS

This work is supported by the European Commission under CP grant no. 248587, "THE Hand Embodied", within the FP7-ICT-2009-4-2-1 program "Cognitive Systems and Robotics".

APPENDIX

Each block $T_{ij}^P \in \mathbb{R}^{6\times 1}$ can be evaluated by the following rule:

- if the $j-$th tendon is neither connected to the $i-$th body, nor it passes through a sheath fixed to it, $T_{ij}^P = 0 \in \mathbb{R}^{6\times 1}$;
- if the $j-$th tendon is connected to the $i-$th link and passes through a sheath fixed to the $k-$th link,

$$T_{ij}^P = \frac{1}{\|p_{k,j} - p_{i,j}\|} \begin{bmatrix} p_{k,j} - p_{i,j} \\ p_{i,j} \times p_{k,j} \end{bmatrix}; \tag{37}$$

- if the $j-$th tendon is connected to/passes through the $h-$th link, passes through the $i-$th link, and is connected to/passes through the $k-$th link,

$$T_{ij}^P = \frac{1}{\|p_{h,j} + p_{k,j} - 2p_{i,j}\|} \begin{bmatrix} p_{h,j} + p_{k,j} - 2p_{i,j} \\ p_{i,j} \times (p_{h,j} + p_{k,j}) \end{bmatrix} \tag{38}$$

REFERENCES

[1] R. Balasubramanian and Y. Matsuoka, "Biological stiffness control strategies for the anatomically correct testbed (ACT) hand," in *Robotics and Automation (ICRA), 2008 IEEE International Conference on*, May 2008.
[2] M. Vande Weghe, M. Rogers, M. Weissert, and Y. Matsuoka, "The ACT hand: design of the skeletal structure," in *Robotics and Automation, 2004. Proceedings. ICRA '04. 2004 IEEE International Conference on*, vol. 4, apr. 2004, pp. 3375 – 3379.
[3] A. Deshpande, J. Ko, D. Fox, and Y. Matsuoka, "Anatomically correct testbed hand control: Muscle and joint control strategies," in *Robotics and Automation (ICRA), 2009 IEEE International Conference on*, May 2009, pp. 4416 –4422.
[4] M. Grebenstein and P. van der Smagt, "Antagonism for a highly anthropomorphic hand-arm system," *Advanced Robotics*, no. 22, pp. 39–55, 2008.
[5] M. Chalon, T. Wimböck, and G. Hirzinger, "Torque and workspace analysis for flexible tendon driven mechanisms," in *2010 IEEE ICRA*, Anchorage, Alaska, USA, May 3-8 2010, pp. 1175 – 1181.
[6] A. Albu-Schäffer, O. Eiberger, M. Grebenstein, S. Haddadin, C. Ott, T. Wimböck, S. Wolf, and G. Hirzinger, "Soft robotics: from torque feedback controlled lightweight robots to intrinsically compliant systems," *IEEE Robotics and Automation Magazine*, vol. 15, no. 3, pp. 20 –30, 2008.
[7] J. Lee and L. Tsai, "The structural synthesis of tendon-driven manipulators having a pseudotriangular structure matrix," *International Journal of Robotics Research*, vol. 10, no. 3, pp. 255–262, 1991.
[8] L. Barbieri and M. Bergamasco, "Nets of tendons and actuators: an anthropomorphic model for the actuation system of dextrous robot hands," in *5−th Int. Conf. Advanced Robotics*, 1991, pp. 357 – 362.
[9] R. Kurtz and V. Hayward, "Dexterity measures with unilateral actuation constraints: the $n+1$ case," *Journal of Advanced Robotics*, vol. 9, no. 5, pp. 561–577, 1995.
[10] S. Fang, D. Franitza, M. Torlo, F. Bekes, and M. Hiller, "Motion control of a tendon-based parallel manipulator using optimal tension distribution," *IEEE/ASME Transactions of Mechatronics*, vol. 9, no. 3, pp. 561–568, 2004.
[11] J. Leijnse and J. Kalker, "A two-dimensional kinematic model of the lumbrical in the human finger," *Journal of Biomechanics*, vol. 28, no. 3, pp. 237–249, 1995.
[12] F. Mussa-Ivaldi, P. Morasso, and R. Zaccaria, "Kinematics networks," *Biol. Cybern.*, vol. 60, pp. 1–16, 1988.
[13] A. Bicchi and D. Prattichizzo, "Analysis and optimization of tendinous actuation for biomorphically designed robotic systems," *Robotica*, vol. 18, pp. 23–31, 2000.
[14] R. W. Brockett, "Robotic manipulators and the product of exponentials formula," in *Mathematical Theory of Networks and Systems*, P. A. Fuhrman, Ed. New York: Springer-Verlag, 1984.
[15] F. C. Park, "Computational aspects of the product-of-exponentials formula for robot kinematics," *IEEE Transactions on Automatic Control*, vol. 39, no. 3, pp. 643–647, Mar. 1994.
[16] R. M. Murray, Z. Li, and S. Sastry, *A Mathematical Introduction to Robotic Manipulation*. Boca Raton, FL: CRC Press, 1994.
[17] D. J. Montana, "The kinematics of contact and grasp," *The International Journal of Robotics Research*, vol. 7, no. 3, pp. 17–32, 1988.
[18] M. Gabiccini and A. Bicchi, "On the role of hand synergies in the optimal choice of grasping forces," in *Proceedings of Robotics: Science and Systems*, Zaragoza, Spain, June 2010.
[19] A. Bicchi, "On the closure properties of robotic grasping," *The International Journal of Robotics Research*, vol. 14, no. 4, pp. 319–334, August 1995.
[20] J. Nocedal and S. J. Wright, *Numerical Optimization*. Springer, August 2000.
[21] H. Borgstrom, M. Batalin, G. Sukhatme, and W. Kaiser, "Weighted barrier functions for computation of force distributions with friction cone constraints," in *2010 IEEE ICRA*, Anchorage, Alaska, USA, May 3-8 2010, pp. 785 –792.
[22] S. Boyd and L. Vandenberghe, *Convex Optimization*. New York, NY, USA: Cambridge University Press, 2004. [Online]. Available: http://portal.acm.org/citation.cfm?id=993483
[23] A. A. Shabana, *Computational Dynamics*, 2nd ed. John Wiley and Sons, 2001.